Brazilian Journal of Geophysics

RBGf

HIGH RESOLUTION IMPEDANCE INVERSION

Carlos Alves da Cunha, Andrea Damasceno, Anderson Luiz Pimentel, Leonardo Marcio Teixeira da Silva,
Nathalia Martinho Souto Muniz da Cruz and Tatiana Alice Soares de Oliveira

ABSTRACT. The identification of clay rich layers is crucial for development of pre-salt reservoirs. They represent flow barriers and compromise the return of investment of the project if the thickness is misvalued. This issue becomes more relevant for thin clay rich layers. The solution for the characterization of thin beds is classic: increase of the frequency bandwidth in seismic data. Here, we present a new methodology to derive high-frequency impedance volume. Our approach starts with the recovery of low and high-frequency components in seismic data by the application of iterative deconvolution (iterdec). Then the extended bandwidth data are employed as input amplitude data to the sparse-spike inversion. The outcome is a high-frequency acoustic impedance volume, which improves the interpretation of thin clay rich layers. We present a study case of a pre-salt reservoir to demonstrate that this technique mitigated the location risk of an injection well and helped to maximize the oil swept of its vicinity. Furthermore, we discuss the required adaptations in the sparse-spike inversion workflow, and present the advantages of this approach when compared to conventional inversion results.

Keywords: inversion, resolution, broadband, pre-salt.

RESUMO. A identificação de camadas argilosas é crucial para o desenvolvimento de reservatórios do pré-sal. Elas atuam como barreira para o fluxo dos fluidos, comprometendo o retorno do investimento no projeto, se sua espessura for subavaliada. Esta questão se torna mais relevante no caso de camadas argilosas de pequena espessura. A solução para a caracterização de camadas finas é clássica: torna-se necessário aumentar a banda espectral do dado sísmico. O presente trabalho apresenta a metodologia e os primeiros resultados da incorporação de uma nova metodologia para geração de volumes de impedância de alta resolução. Nesta abordagem, os componentes de baixa e alta frequência do dado sísmico são recuperados através da aplicação de um processo de deconvolução iterativa (iterdec). Em seguida, estes dados, com banda espectral expandida, são utilizados como entrada para uma inversão esparsa, resultando num volume de impedância acústica, que reduz as incertezas na interpretação de camadas argilosas de pouca espessura. Apresenta-se o estudo de caso de um reservatório do pré-sal para demonstrar a efetividade desta técnica na mitigação de risco associado ao posicionamento de um poço injetor, resultando na maximização da varredura de óleo em torno do poço. São apresentadas e discutidas as adaptações necessárias ao fluxo tradicional de inversão e condicionamento de dados sísmicos, bem como as vantagens da aplicação dessa metodologia em comparação com os resultados da inversão.

Palavras-chave: inversão, resolução, banda-larga, pré-sal.

Corresponding author: Carlos Alves da Cunha
Petrobras, Av. Chile 220, 12º andar Torre Leste, Centro, 20031-912 Rio de Janeiro, RJ, Brazil – E-mails: ccunha@petrobras.com.br, adamasceno@petrobras.com.br, andersonp@petrobras.com.br, lmtsilva@petrobras.com.br, nathalia.martinho@petrobras.com.br, tatiana.alice@petrobras.com.br

INTRODUCTION

During the last two decades, internal research inside Petrobras led to the development of a suite of processes to improve the resolution of seismic volumes. Applications of these processes were limited to the universe of qualitative applications in which faciologic, lithologic and fluid characterization are described in terms of relative physical quantities. These applications include internal publications regarding the characterization of carbonate reservoirs of pre-salt in Santos basin and 4-D analysis of turbidities in Campos basin, facies mapping of the pre-salt reservoirs in Campos basin (Cunha et al., 2013).

On the other hand, advances on seismic acquisition and processing improved the reliability of the seismic amplitude; thereby the quantitative interpretation of turbidite and pre-salt reservoirs based on impedance volumes became more trustworthy and integrated with static and dynamic data (Teixeira et al., 2017). However, conventional impedance volumes are restricted to the bandwidth of the input data and, therefore, have not benefited from the bandwidth expansion processes.

Seismic quantification of rock properties relies on the combination of rock physics and seismic inversion (Avseth et al., 2005; Vernik, 2016). Rock physics links the petrophysical and elastic properties. It evaluates how saturating fluid, porosity, clay content, pore shape, mineralogy, and pressure affects the seismic signal. Sparse-spike seismic inversion enables the spatial extrapolation of well-derived elastic properties by inverting the migrated traces into elastic properties (Latimer, 2011). The incorporation of low and high frequencies in the bandwidth of the seismic inversion process, significantly improves reservoir characterization, with quantitative characterization of the depositional system geometry, and rock properties with resolution more compatible with the scales involved in flow simulations.

ITERATIVE DECONVOLUTION AND HIGH RESOLUTION PSEUDO-IMPEDANCE

The bandwidth of seismic data imposes a limit to our capacity to resolve stratigraphic features associated with facies characterization in a reservoir scale. Several methods usually referred to as sparse-spike deconvolution (or inversion), aim to loosen this limitation by the expansion of the frequency bandwidth (Debeye & van Riel, 1990; Velis, 2008; Zhang & Castagna, 2011; Liang et al., 2017).

This process of residual deconvolution of the seismic wavelet from migrated volumes, which provides reflectivity volumes with an expanded frequency bandwidth, has also a long history of development in Petrobras. Internally known as iterative deconvolution (iterdec), its origin remotes to the late 1970's, originally formulated by José Tassini and Emilson Evangelista, and subsequently improved by André Romanelli (Rosa, 2018). This process was subject to several refinements along the last two decades, with developments that include the stage of data pre-conditioning (Machado & Cunha, 2015), further improvement of the as well as the deconvolution process itself, and the post-conditioning stage.

The pre-conditioning stage comprises attenuation of coherent and incoherent noises as well as residual phase correction of the wavelet. The phase correction uses seismic/synthetic fitting at well locations as well as the analysis of other reference events such as the water bottom and igneous intrusions.

Figure 1 illustrates the residual phase correction for the case of using the water bottom event as reference. By adjusting a linear trend to the relevant part of the phase spectrum, it is possible to determine the phase rotation that provides a null linear coefficient. In the particular case of this dataset, a phase rotation of 20° was necessary. Subsequent correlation with synthetic traces at well locations validated this correction.
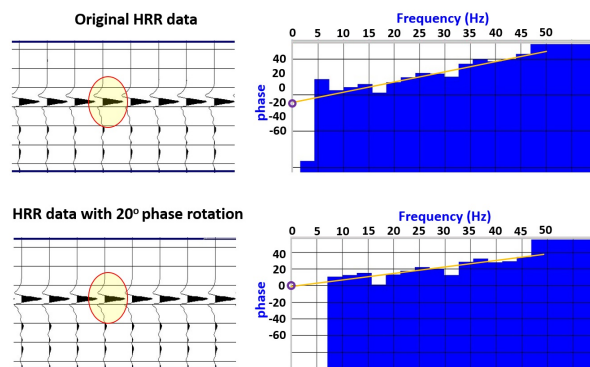
Figure 1 – Estimating the residual phase correction. Top: HRR data without phase rotation and their average phase spectrum. Bottom: HRR data after 20° phase rotation and their average phase spectrum. The phase rotation corrects the wavelet asymmetry observed in the original data.

After the residual wavelet deconvolution, it is necessary to simulate the spectral tendency of the subsurface reflectivity series. This is achieved by a spectral coloring shaping procedure, as described in (Rosa & Ulrych, 1991). The spectrally shaped deconvolved data are then subject to time integration, which simulates a conversion from reflectivity to relative impedance. The next stage involves a process called High Resolution Pseudo-Impedance (PSIM) filter, which consists of a combination
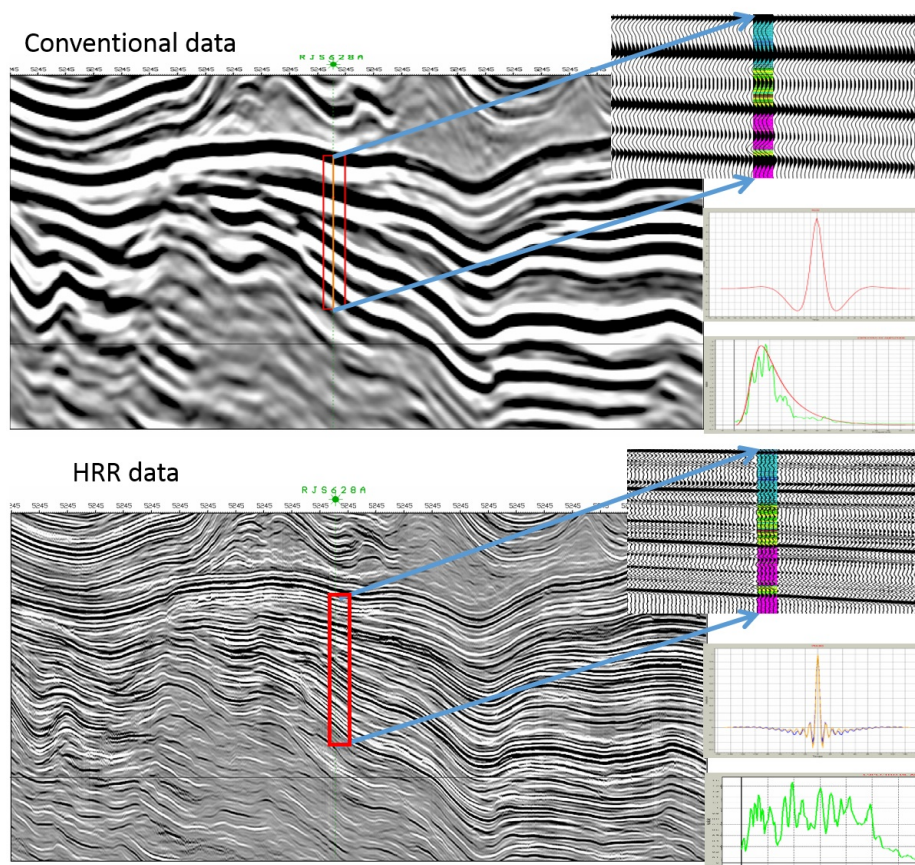
Figure 2 – Top: Conventional data. Bottom: HRR data. Amplified windows show good correlation of both with respective well-derived synthetics (each with their own wavelet).

of temporal and spatial structural filters that aim at the attenuation of the low-frequency noise amplified by the integration. This process preserves the low-frequency signal, which is normally discharged in conventional filtering processes. Finally, we differentiate the PSIM data with respect to time, resulting in a High Resolution Reflectivity (HRR) volume.

Figure 2 compares the (conventional) input data and the HRR data for 2-D window around Well-1. We verify the expressive increase in resolution, with continuous reflectors free from the usual artifacts amplified by typical processes of spectral enhancement, while preserving good correlation with the synthetic traces.

Inversion of the High Resolution Data

From the 47 wells used in this project, 25 show a seismic-log correlation higher than 60% for the high resolution data, considering a time window comprising the entire log length.

The Time/Depth calibration for broadband data is still more critical than that for conventional data, since a small mismatch produces a significant decrease in the synthetic/seismic cross correlation due to the bandwidth expansion. In order to cope with this problem we developed an internal tool that performs automatic seismic-log tie, based on running correlation maximization, after the usual manual adjustments of the drift.

Regarding the seismic wavelet estimation, it is important to realize that the usual tools provided by commercial inversion software, which are based on least squares minimization between seismic and synthetics were not developed for broadband data. This method is efficient to estimate wavelets for conventional data, but inadequate for high resolution data, such as HRR.

First, we need to readdress the time window length required for the wavelet estimation. For a satisfactory estimation of the amplitude spectrum, this length needs to be at least three times the length of the wavelet, especially to capture the amplitudes
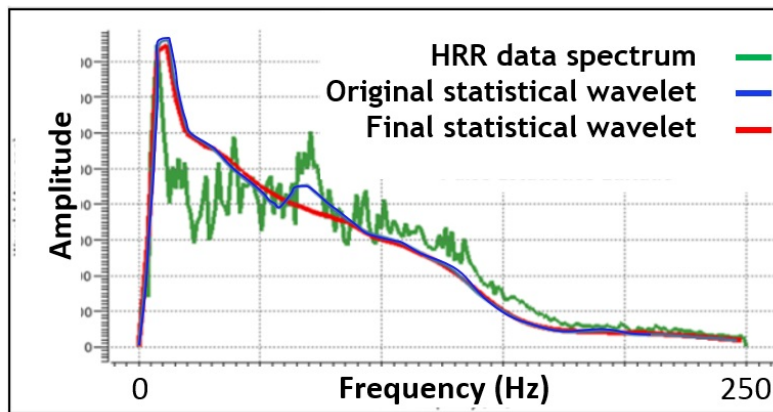
Figure 3 – Comparing seismic spectrum (green) with original statistical wavelet (blue) and its edited version (red).
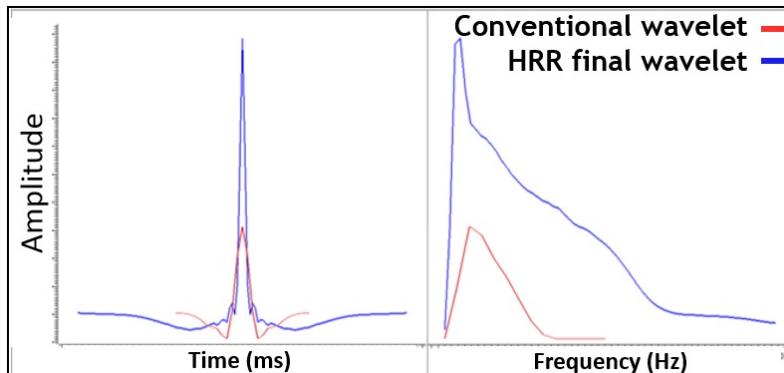
Figure 4 – Superposition of final estimated wavelets for conventional data (red) and HRR data (blue). The HRR wavelet is broader, allowing for more low-frequency content and with much smaller side lobes.

associated with the low frequencies. However, in this project, as in most standard projects, sonic and density logs have a limited depth range, which may be inadequate even for conventional data. To cope with these issues, we opted for an alternative strategy, with a combination of automatic tools and manual adjustments.

The first step of the wavelet estimation is purely based on seismic data (without any well-related information). The use of a large number of traces, with a larger time window than that usually involved in conventional inversion, allows for a more robust estimation. Figure 3 compares the average seismic spectrum, the seismic derived statistical wavelet spectrum, and a manually edited version of the wavelet spectrum to produce a smoother version. The next step comprises the least squares adjustment of phase and amplitude, using the edited statistical wavelet as *a priori* information with strong *a priori* weight. In this approach, the

only purpose of the least squares adjustment is to guarantee that the seismic amplitudes honor the amplitude from the synthetics derived from the well logs. The phase correction was neglectable and thus set to zero.

Figure 4 shows the final wavelets estimated for the conventional and the high resolution data, as well as their corresponding amplitude spectra.

The inversion parametrization had also to be adapted to cope with the differences between the high resolution data and conventional data. The main characteristics of the high resolution data that interfere with the inversion parametrization are:

- Lower noise content;

- Larger number of significant reflectors;

- Reliable signal down to a frequency of 4 Hz.
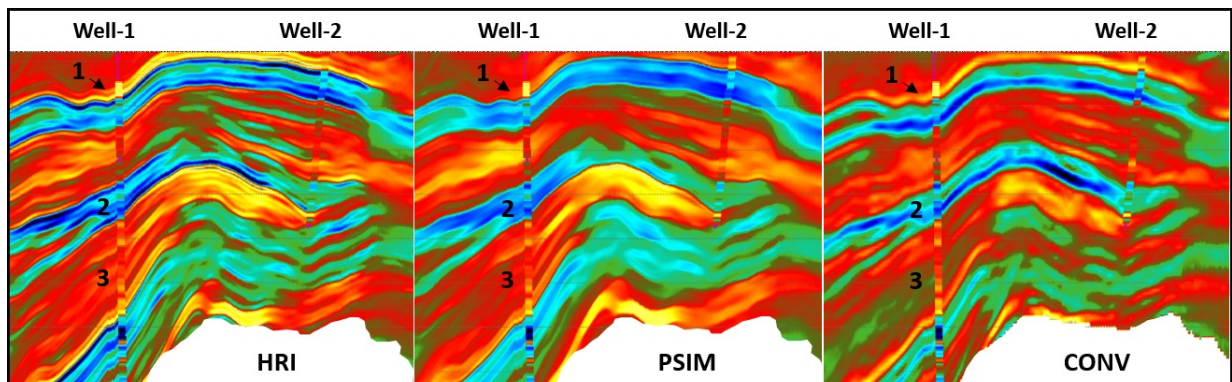
Figure 5 – Results from three different approaches to acoustic inversion for a section crossing two wells. Hot colors (yellow to red) correspond to low impedances, while cold colors (light green to dark blue) correspond to high impedances. A trapezoidal band-pass filter (3.5 Hz-5.5 Hz-137 Hz-162.Hz) was applied to the seismic traces as well as to the well logs. We verify that the HRI approach shows better correlation with the well logs when compared to the other two approaches.

The sparse-spike inversion conceives lateral continuity to provide smoother results. Furthermore, we follow a two-step approach (Sobreira & Damasceno, 2014 – internal report) for the low-frequency insertion. This proposal counts on two-inversion scheme. The acoustic impedance from the first inversion is filtered and used as low-frequency trend in the second inversion. As a result, stratigraphic features became more laterally continuous, removing subvertical artifacts. We used merge frequencies of 4 Hz in the first step and 12 Hz in the second step.

ANALYSIS AND QUALITY CONTROL OF RESULTS

The results were analyzed in 1-D, by comparing the inverted traces with the logs at the well positions, and in 2-D, by comparing the seismic section along the wells. We also compare the acoustic impedance derived from the sonic and density logs with three versions of the inversion: conventional inversion (CONV); pseudo-impedance inversion (PSIM), derived from the integration of the high resolution data (which lacks very low-frequency components) and the high resolution inversion (HRI), which blends the iterative deconvolution large bandwidth seismic and the sparse-spike seismic inversion. Finally, we show the results of blind wells.

Pseudo-wells and sections

To illustrate the concept that the high resolution inversion produces superior results (as compared to conventional inversion), not only in terms of better resolution, but also, in terms of more reliable absolute values of amplitudes we constructed Figure 5. It compares the results from three inversions: Conventional, PSIM, and HRI. For a section, that crosses two wells (Well-1 and Well-2). Inspecting this figure, we verify that:

The transitions among layers are smoother in the conventional inversion. The more abrupt contrast shown in the other two inversions is more geologically consistent with the discontinuous character of stratigraphic units.

The HRI is capable to identify the thin (10 m) anhydrite layers (dark blue in region 1), and although it is present also in PSIM its amplitude (tonality) shows a small relative contrast. We observe a similar behavior in other high relative impedance features (dark blue layers) in region 2, as well, in region 3.

The smaller (seismically related) content of low frequencies in the conventional inversion produces incorrect amplitudes (greenish colors) in thicker layers, such as in the Piçarras formation indicated in the region 3, as attested by the well log.

The dark blue feature in region 2 would be interpreted as a single body in the conventional inversion, but as three independent bodies (and more conform to local layer attitudes) in the HRI.

In general, the HRI combines the stratigraphic details provided by the PSIM inversion with a more rigorous amplitude control provided by the sparse-spike inversion methodology.

To complement these observations, Figure 6 compares impedance logs (full bandwidth up to 175 Hz) of Well-1 and the traces from the HRI and CONV inversions. A visual inspection shows that (except for the last 50 ms) the HRI correlates better with the well log than the CONV inversion. The superiority holds in quantitative terms: 0.9 for HRI and 0.84 for CONV. It is worthwhile to point that this result is even more surprising when we consider
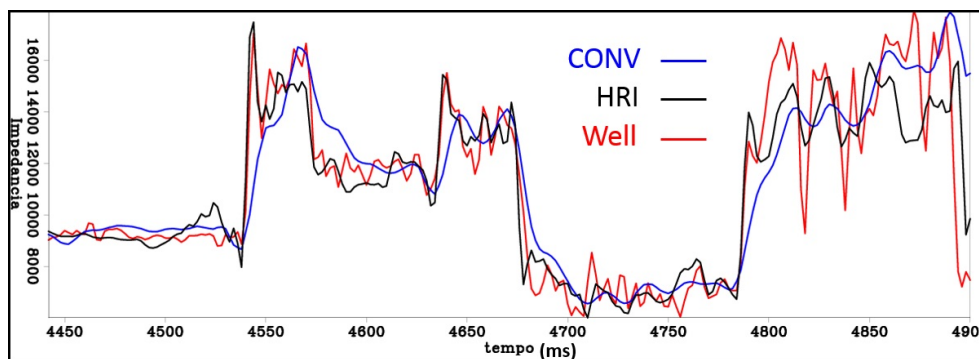
Figure 6 – Acoustic Impedance logs: (red) from Well-1; (blue) from conventional inversion; (black) from high resolution inversion. The HRI result reproduces the sharp impedance contrasts present in the well log for a bandwidth up to 175 Hz.
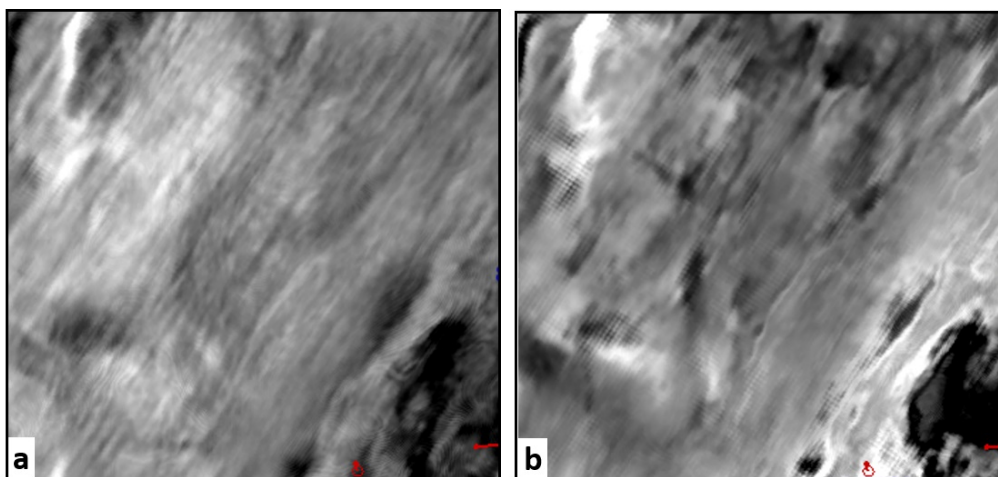
Figure 7 – Strata slice near the top of reservoir. (a) Conventional inversion; (b) HRI.

that the CONV inversion used more information from the well (up to 6 Hz) than the HRI (up to 4 Hz), since Well-1 was used for the low-frequency model.

Maps – Horizon slices

Figure 7 presents a map comparison of the two inversion results. They correspond to a strata slice extracted near the top of the reservoir.

The HRI provides better focusing of all the features in the strata slice, improving the definition of layer boundaries, and the identification of stratigraphic units.

Blind Tests

We selected five wells to use as blind tests (not used in any part of the inversion workflow). We present, for each of the wells in Table 1, two values of correlation with the seismic inversions at the well locations. Values on the left correspond to full bandwidth, and on the right (bold face) with a low cut of 6 Hz.

Table 1 – Correlation values (in %) between well log acoustic impedances and seismic inverted traces for the two approaches: CONV and HRI. Values on the left correspond to full bandwidth, and on the right (bold face) with a low cut of 6 Hz.

Well	Well-3		Well-4		Well-5		Well-6		Well-7	
CONV	75	**51**	60	**44**	90	**50**	87	**73**	89	**71**
HRI	79	**63**	60	**45**	95	**72**	79	**80**	91	**80**

Because the insertion of the low frequencies derived from wells involved different merge frequencies, presenting the values with the 6 Hz low cut allows for a comparison in a bandwidth less susceptible to the influence of the well-derived low-frequency model.
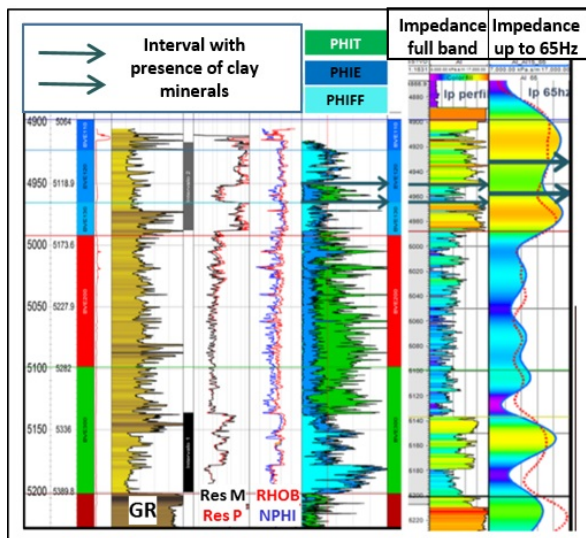
Figure 8 – On the left several logs showing a layer with clay minerals indicated by the interval between the two arrows. On the right two versions of the well-based acoustic impedance, one in full bandwidth, and the other with a 65 Hz high-cut filter. We verify that the limitation of the bandwidth decreases the resolution of the clayish layer not only in terms of impedance contrast (amplitude) but also in terms of thickness and positioning.

Figure 9 – Inversion results for a section crossing Well-15. (a) Conventional inversion; (b) HRI; (c) detail of (a) with interpretation and 65 Hz high-cut impedance profile from well; (d) detail of (b) with interpretation and "full-band" impedance profile from well.

POSITIONING AN INJECTOR AT A BORDER OF THE FIELD

The distance between injectors and producers should be as large as possible in order to optimize the injected fluid pathways inside the reservoir, enhancing the oil production, and avoiding premature water breakthrough.

The best positions for injector wells are typically located in lower structures of reservoirs to maintain the pressure and optimize the oil sweep by differential density and gravity. The lake bathymetry is a key control for facies deposition of pre-salt reservoirs (Faria et al., 2017). Therefore, positioning injector wells in lower structures increases the risk of drilling clay-bearing carbonate facies, penetrating low porosity and permeability rocks.

Therefore, an important part of the geological characterization of pre-salt reservoirs is the prediction of the most probable regions where non-reservoir facies are present, and where respective transition zones, from clear to clay-bearing carbonates, occur, in order to optimize the drainage.

Figure 8 presents some logs from Well-15, which is located at a region characterized by the occurrence of transitional facies, near the west border of the field. The arrows in the figure indicate a zone of low permoporosity due to the presence of clay minerals in the carbonate rocks. The borders of the field studied here are comprised by facies with low permoporosity due to a high content of clay minerals.

A section across this well presents the results from the conventional and the high resolution acoustic inversions (Fig. 9). The gain of resolution achieved with the HRI approach significantly reduces the uncertainties to characterize the geometries of the two facies involved.

In addition to a better delineation of the clay-bearing carbonate lens, the high resolution inversion is more effective to identify the lateral facies transition characterized by interdigitation of associated facies. The high permoporosity reservoir zone (dark blue) as well as the thin clay rich layer (light blue to green) are better defined, and with a geometry more geologically consistent in the HRI than the CONV inversion.

The gradual interdigitation between the two facies becomes evident. Although the conventional inversion fits reasonably the band limited well log impedance, it leads to an inaccurate description of zone 1, as previously discussed. On the other hand, the high resolution inversion adjusts well the "full band" impedance profile from the well, leading to a more accurate and geologically meaningful image.

Integrated studies of flow simulation, risk analysis for the presence of clay minerals at the reservoir and economic
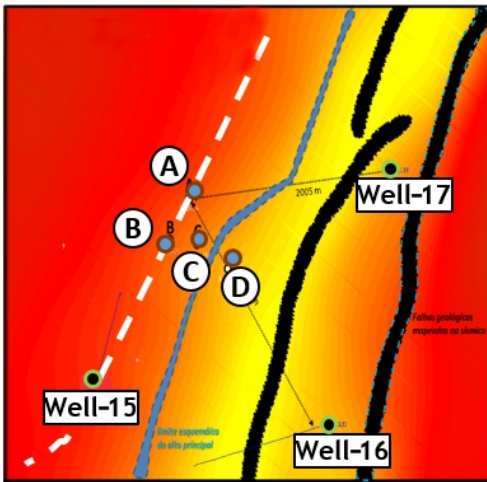
Figure 10 – Location map of the four possible locations for the additional injector well. The location of two production wells and one injector well are also marked.
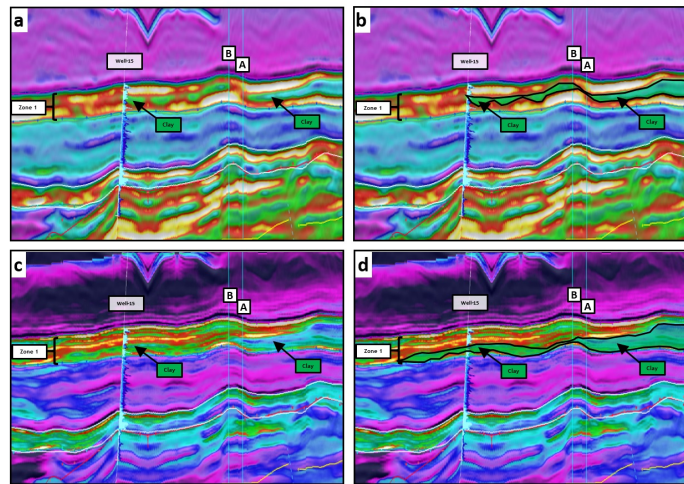
Figure 11 – Arbitrary section indicated by the white dashed line in Figure 10. a) Conventional inversion; b) Conventional inversion with delineation of the clay-bearing carbonate layer; c) High resolution inversion; d) High resolution inversion with delineation of the clay-bearing carbonate layer. The clay-bearing intervals becomes more continuous and geologically consistent in the high resolution inversion.
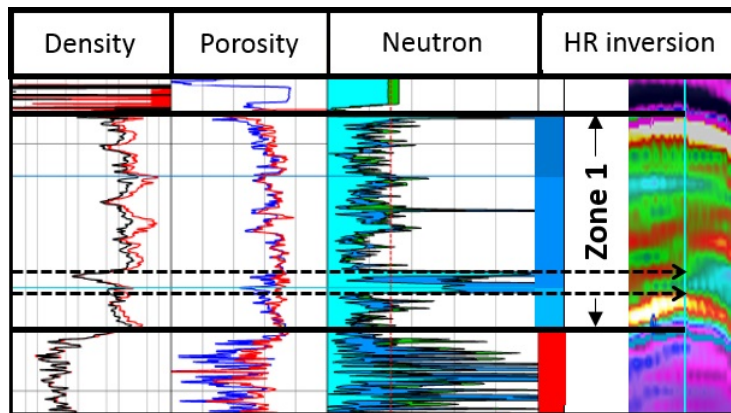
Figure 12 – A suite of borehole logs for the well drilled at location B. The two horizontal solid black lines are the boundary of zone 1. The two horizontal dashed black arrows delimit the clay rich carbonate lens. Both the thickness and position of the clay rich layer are in good agreement with the HRI image at the well location.

analysis, led to the selection of four possible locations for the new injector. Figure 10 presents a map of these locations, along with injector Well-15, and production wells 16 and 17. Flow simulations favored two locations, while geological risk analysis recommended the other two locations.

It became critical to perform a detailed study using the high resolution data to reduce the geological uncertainty and support a safe location in a position better suited for the drainage optimization.

Figure 11 compares positions A and B with Well-15 along the white dashed line in the map of Figure 10. The benefit of evaluating the well position in the high resolution data becomes evident. Can we not only testify the progression of the clay dominant strata, but also predict that a well in position B would drill the same thickness of this stratum as encountered in Well-15. Based on lateral seismic facies association, the net porosity of zone 1 should not compromise the requirements of the project. After drilling the well at location B, we verified that the position

and thickness of the clay rich layer confirmed the predictions based on the HRI, as shown in Figure 12.

In addition to improve the definition of the boundaries of the clay rich carbonate lenses, the HRI became an important tool to better understand the lateral transition of facies, resulting in a more geologically consistent map of the associated facies interdigitation.

FINAL COMMENTS AND CONCLUSIONS

We presented the general workflow for producing high resolution reflectivity (HRR) volumes. We also discussed the required adaptations in the conventional inversion workflow in order to cope with the particularities of the HRR data.

To evaluate the results we compared three inversion approaches: conventional inversion, pseudo-impedance inversion and high resolution inversion. The advantages of this new methodology are quite representative, as demonstrated by the sections across some wells. Both, the well data and the quality control result support the improvement in resolution attained with the HRI. Blind tests also attest the capability of HRI to capture high-frequency information from seismic.

The use of the HRI volume supported the location of new injectors and producers in the field. This approach significantly enhances not only in the characterization of the reservoir internal geometries (and the associated depositional system), as well as in quantitative estimation of reservoir properties with resolution more compatible with flow simulation models.

ACKNOWLEDGMENTS

REFERENCES

AVSETH P, MUKERJI T & MAVKO G. 2005. Quantitative seismic interpretation: Applying rock physics tools to reduce interpretation risk. Cambridge University Press. 376 pp. doi: 10.1017/CBO9780511600074.

CUNHA CA, RUTHNER MP, GONTIJO RC & ALMEIDA SHM. 2013. Statistical Seismic Facies Estimation from Pseudo Impedance Data. In: 13th International Congress of the Brazilian Geophysical Society. Rio de Janeiro, RJ, Brazil: SBGf. doi: 10.1190/sbgf2013-131.

DEBEYE HWJ & VAN RIEL P. 1990. Lp-norm deconvolution. Geophysical Prospecting, 38: 381-403. doi: 10.111/j.1365-2478.tb01852.x.

FARIA DL, REIS AT & SOUZA JR OG. 2017. Three-dimensional stratigraphic-sedimentological forward modeling of an Aptian carbonate reservoir deposited during the sag stage in the Santos Basin, Brazil. Marine and Petroleum Geology, 88: 676-695. doi: 10.1016/j.marpetgeo.2017.09.013.

LATIMER RB. 2011. Inversion and interpretation of impedance data. In: BROWN AR. Interpretation of Three-Dimensional Seismic Data. Society of Exploration Geophysicists and American Association of Petroleum Geologists. 7th ed., chapter 9, p. 309–350. doi: 10.1190/1.9781560802884.ch9.

LIANG C, CASTAGNA J & TORRES RZ. 2017. Tutorial: Spectral bandwidth extension – Invention versus harmonic extrapolation. Geophysics, 82: W1-W16. doi: 10.1190/GEO2015-0572.1.

MACHADO M & CUNHA C. 2015. Structure-oriented Filter by Domain Decomposition. In: 14th International Congress of the Brazilian Geophysical Society. Rio de Janeiro, RJ, Brazil: SBGf. p. 1285-1290.

ROSA ALR. 2018. Análise do Sinal Sísmico. 2nd ed., Rio de Janeiro, Brazil: SBGf. 713 pp.

ROSA AR & ULRYCH T. 1991. Processing via spectral modeling. Geophysics, 56(8): 1244-1251. doi: 10.1007/s12182-009-0024-x.

SOBREIRA M & DAMASCENO A. 2014. Inversão elástica em duas passadas: ganhos de resolução e menor dependência dos poços. Brazil. Internal Report.

TEIXEIRA L, CRUZ N, SILVANY P & FONSECA J. 2017. Quantitative Seismic Interpretation integrated with well-test analysis in turbidite and presalt reservoirs. The Leading Edge, 36(11): 931-937.

VELIS DR. 2008. Stochastic sparse-spike deconvolution. Geophysics, 73: R1-R9. doi: 10.1190/1.2790584.

VERNIK L. 2016. Seismic petrophysics in quantitative interpretation. Houston, TX. Society of Exploration Geophysicists (SEG). 226 pp. doi: 10.1190/1.9781560803256.fm.

ZHANG R & CASTAGNA J. 2011. Seismic sparse-layer reflectivity inversion using basis pursuit decomposition. Geophysics, 76: R147-R158. doi: 10.1190/GEO0211-0103-1.